

# Hybrid Wing-Body Aircraft Landing Gear Design

Phillip W. Richards<sup>1</sup> and Boone Tate<sup>2</sup>  
*SDI Engineering Inc., Bellevue, WA, 98005, USA*

This paper details the design considerations for landing gear of hybrid wing-body (HWB) aircraft. This includes landing gear locations, weight distribution, leg and axle dimensions, tire selection, and oleo properties. Traditional landing gear placement, in which the main gears are located very closely to the center of mass, and thus bearing the majority of the load distribution, is oftentimes not feasible in HWB aircraft due to unique geometric constraints. Given these design considerations, SDI Engineering has created detailed landing gear models for multiple HWB aircraft designs within GearSim, a proprietary landing gear and aircraft modeling and analysis software tool. These models provide loading information about the various landing gear components which were then compared to similarly sized traditional aircraft models. Results from these simulations show that for larger HWB aircraft, the landing gear configuration and design can be similar to traditional large aircraft such as the B777 or A380. However, for smaller HWB aircraft, the nose landing gear (NLG) must be designed to carry a larger proportion of the load during regular aircraft operations. This can be overcome by the use of larger tires, or a four-wheel NLG that is discussed in further detail. The methods presented in this paper can be used by future landing gear and subsystem design engineers to better optimize landing gear for more detailed HWB aircraft designs in the future.

## I. Nomenclature

BWB	=	blended wing-body
CFD	=	computational fluid dynamics
CG	=	center of gravity
FW	=	flying wing
HWB	=	hybrid wing-body
LG	=	landing gear
MLG	=	main landing gear
MTOW	=	maximum takeoff weight
NBC	=	narrow-body commercial
NLG	=	nose landing gear
SDI	=	SDI Engineering Inc.
WBC	=	wide-body commercial

## II. Introduction

Flying wing (FW), blended wing-body aircraft (BWB), and hybrid wing-body aircraft (HWB) have been extensively studied by the aerospace community in recent decades, particularly driven by the promise of increased efficiency in commercial/passenger applications [1, 2, 3, 4, 5, 6, 7]. Numerous authors have attempted preliminary and conceptual studies of FW, BWB, and HWB designs that meet range, passenger capacity, and/or efficiency requirements [8, 9, 10, 11, 12, 13, 14]. Other authors have investigated the specifics behind the structural and aerodynamic design of these aircraft, including structural optimization [15, 16, 17, 18] and wind tunnel testing/computational fluid dynamics (CFD) [13]. However, the configuration and placement of the landing gear (LG) systems in these design studies is at best an afterthought, if included at all [19]. For example, design guidelines have been used for conventional tube and wing aircraft for a BWB [11]. While these aircraft potentially represent the future of commercial air travel, they also have unique design considerations and requirements for the nose and

---

<sup>1</sup> Principal Engineer, AIAA Member.

<sup>2</sup> Mechanical Engineer.

main landing gear (NLG, MLG) that differ dramatically from the requirements posed by the typical tube-and-wing aircraft construction.

In both potential configurations, the HWB structure must contain space for passengers/cargo, fuel and other critical systems like avionics. This is in contrast to a tube-wing design in which fuel largely occupies the wings and small portions of the fuselage; and passengers/cargo, landing systems and systems such as avionics that share the fuselage space. The different space constraints, combined with the unique geometries and lofts of a FW or BWB aircraft, creates unique restrictions on landing gear placement and stowage, and loading conditions.

In the proposed designs thus far, authors have categorized the wide range of HWB aircraft into three families. For mid-sized HWB aircraft, referred to as HWB2, there is enough fuselage height for a second deck below the main passenger deck. In this case, the landing gear can be placed and designed similar to conventional aircraft, with no major difference between the LG design process between these aircraft and the conventional aircraft. For very large aircraft, referred to as HWB3, a large number of landing gear are required, and the design requirements are similar to large military transport aircraft. For example, in [20], a four-wheel NLG and four-wheel MLG are depicted, which is the same arrangement as a C-5 aircraft. For smaller HWB aircraft, referred to as HWB1, when the weight is on the order of a narrow-body commercial aircraft such as the B737 or A320, stowage restrictions force the MLG at a significant distance aft of the center of gravity. This study compares these aircraft to an example narrow-body commercial (NBC) aircraft, which is representative of a B737 or A320, and an example wide-body commercial (WBC6) aircraft, with a six-wheel MLG representative of a B777 or A380. Images of the HWB1, HWB2, and HWB3 aircraft are shown in Fig. 1, based on References [20, 21, 22]. A summary of the aircraft used in this study is presented below in Table 1.

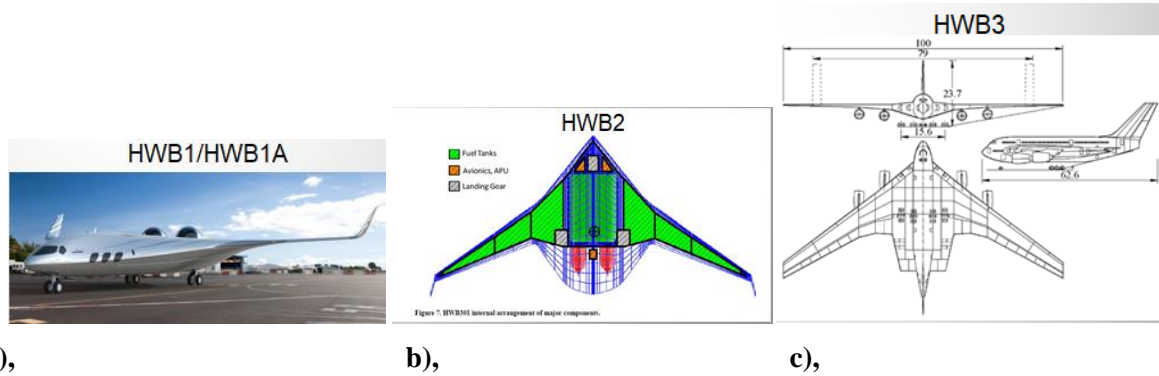


**Fig. 1 Visualization of HWB1/HWB1A (a), HWB2 (b) and HWB3 (c) concepts.**

**Table 1 Summary of considered aircraft types.**

Aircraft	NBC	HWB1	WBC6	HWB2	HWB3	C-5
Seats	200	160	350	300	750	-
Mass, kg	73,500	73,500	251,000	251,000	572,000	378,000
Fuselage Length, m	44.7	24.6	63.7	36.0	62.6	75.5
Span, m	64	53	65	78	100	68
# MLG	2	2	2	2	4	4
LG Type	2	2	6	6	6	6
# MLG Wheels	4	4	12	12	24	24

This work provides a realistic characterization of the landing gear for these three families of systems. For the smaller class of HWB with aft MLG placement, a more detailed design is presented, including overall arrangement, tire selection, oleo shock absorber design, and a preliminary weight estimate. The designs were compared and evaluated for their landing, braking and steering performance. The design, analysis, and simulation of the HWB LG was performed using GearSim, a software tool developed by SDI Engineering Inc. (SDI). SDI previously developed GearSim for loads and subsystems analysis for commercial and military aircraft landing gear [23, 24, 25].

### III. GearSim Landing Gear Analysis and Library Examples

GearSim’s holistic approach to modeling the aircraft and landing gear [23, 24, 25] captures the important nonlinearities and creates a realistic simulation. This enables engineers focused on the individual subsystems such as tires, brakes, and hydraulic system to understand the realistic loading environment, and accurately predict the performance. GearSim’s modular simulation environment enables replacement of individual subsystems with user-created “black-box” models that can enable accurate modeling of proprietary subsystems without sharing the source code with SDI. GearSim is also an ideal platform to study novel concepts or complicated landing maneuvers; for example, aft-wheel steering, off-runway operations, and carrier landings are topics that have been studied using GearSim [24].

GearSim contains library examples that include generic Narrow-Body Commercial (NBC), Wide-Body Commercial (WBC), and Wide-Body Commercial 6-Wheel (WBC6) aircraft as shown in Fig. 2. These aircraft models were used to provide mass, inertia, geometry, and tire properties for use in the sample calculations shown below. The NBC model was also used in full-fidelity simulations, where it is compared to the HWB1 concepts.

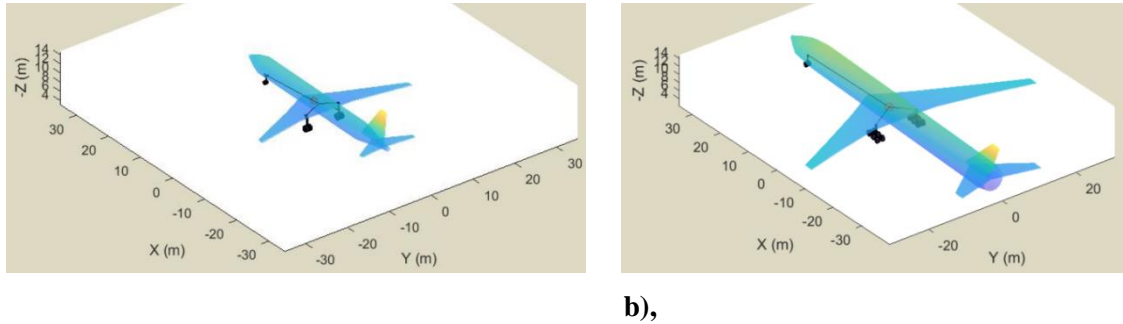


Fig. 2 Visualization of narrow-body (a) and wide-body 6-wheel (b) aircraft models.

### IV. LG Layout and Configuration

For very large HWB aircraft, the landing gear includes a large MLG arrangement placed near or beneath the aircraft’s CG. The size of aircraft and placement of the MLG beneath the CG results in large MLG structures with numerous tires. If most of the weight is carried by the MLG, then the NLG can be designed to be lightweight. This is the case with conventional aircraft, with the design loading condition coming from a maximum braking case where the NLG is resisting a pitch down moment caused by the drag force of the MLG brakes. See Table 2 for a comparison of weight distributions for example HWB2 and HWB3 designs; the tire loads for HWB2 and HWB3 are compared to the WBC6 tire load. These results indicate that the LG design process is similar to that of the WBC6 aircraft.

Table 2 Comparison of LG weight distributions for midsize and large HWB aircraft.

Aircraft	WBC	HWB2	HWB3
Mass, kg	251,000	251,000	572,000
NLG X Position, m	28.67	12.75	22.43
MLG X Position, m	-2.55	-1.1	-1.43
NLG Load, N	201,118	200,420	142,981
NLG Tire Load, N	100,559	100,210 (-0.3%)	84,170 (-16.3%)
MLG Load, N	1,130,596	1,130,945	1,320,090
MLG Tire Load, N	188,433	188,491 (+0.0%)	220,015 (+16.8%)

For HWB designs without sufficient space in the main fuselage section to store the LG, the MLG are placed at the aft portion of the aircraft. The benefits of this configuration are a reduced load demand on the MLG and freeing of space in the aircraft's main body for passengers, cargo, or fuel. However, this has implications for load distribution, ground handling characteristics and takeoff. A larger percentage of the weight on the NLG would result in a relatively larger NLG and smaller MLG. See Table 3 for a comparison in weight distributions for NBC and HWB configurations, with HWB0 being typical of the smallest end of the sizing study in [22], and HWB1/HWB1A representing the Ascent 1000 as described in [21]. These data show a significant increase in NLG tire load for the HWB configurations compared to the NBC. To address this, a 4-wheel NLG design is also shown in [26], which is referred to as HWB1A.

**Table 3 Comparison of LG weight distributions for single-deck HWB aircraft.**

Aircraft	NBC	HWB0	HWB1 (2-Wheel NLG)	HWB1A (4-Wheel NLG)
Mass, kg	73,500	73,500	73,500	73,500
NLG X Position, m	16.23	8.29	9.2	9.2
MLG X Position, m	-1.20	-3.36	-4.9	-4.9
NLG Load, N	49,641	208,056	250,795	250,795
NLG Tire Load, N	24,820	104,028 (+319%)	125,397 (+405%)	62,699 (+153%)
MLG Load, N	335,697	256,490	235,120	235,120
MLG Tire Load, N	167,849	128,245 (-24%)	117,560 (-30%)	117,560 (-30%)

LG configurations with increased track and wheelbase also restrict ground maneuverability. This is based on past experience with large wheelbase traditional aircraft such as the B777 series, which alleviated the issue with aft wheel steering [26]. Additionally, the extreme aft position of the MLG poses a challenge in rotating the aircraft upon takeoff roll, as the position of the LG is level or sometimes aft of the position of the primary flight control surfaces. This rotation issue is addressed in [21] with automatically extending NLG for takeoff, but without any mention to the effect on the landing performance. The effect of braking and steering performance of the novel LG layout will be examined in this study.

## V. Subsystem Design

The subsystem design consists of the tire selection, wheel assembly, oleo-pneumatic shock absorber, and leg structure. The design process mirrors the load path of structural loads from the grounds to airframe, because the primary design variable for each subsystem is the applied load.

The tire selection process for HWB1 and HWB1A began with the static loads on the aircraft tires. Based on a precedent established with the NBC and WBC6, the tire static load was multiplied by a safety factor of 1.6 to determine a required rated load for each tire. The tire stiffness was then determined by comparing the rated load and assuming a damping ratio of 0.1 when supporting that load. Tire weight was also estimated, using the ratio of the tire diameter and width. The tire weight was summed for the NLG tires; the total mass of the four HWB1A tires have a lower total mass than the two HWB1 tires. The results of the tire selection are shown in Table 4.

**Table 4 Tire selection for HWB1 and HWB1A compared to NBC.**

	HWB1 NLG	HWB1A NLG	HWB1 MLG	NBC NLG	NBC MLG
Tire Size	20.00-20	35x11.5-16	44.5x16.5-18	30x8.8	49x18.0-22
Tire Diameter, in	56	35	45	30	49
Tire Width, in	20.1	12	17	9	18
Tire Mass, kg	342	122	223	82	268
Total Mass, kg	684	489	446	164	536
Stiffness, N/m	1,380,165	1,464,621	1,908,335	1,260,000	2,350,000
Damping, N*s/m	8,481	6,178	9,656	3,605	12,804
*Note: NBC tire stiffnesses are for rough reference. HWB1 values are from Goodyear Databook [27].					

Comparing the images for the HWB1 and HWB1A NLG in Fig. 3, large NLG tires would create additional stowage problems. HWB1 and HWB1A also have additional lateral stowage capacity because of the hybrid wing body shape. These stowage considerations along with the weight comparison discussed above imply the 4-wheel NLG design may be a viable strategy for this concept, with a higher static load on the NLG. Another alternative would be two NLG; this option was not considered for this study but can be evaluated as part of a future work effort.

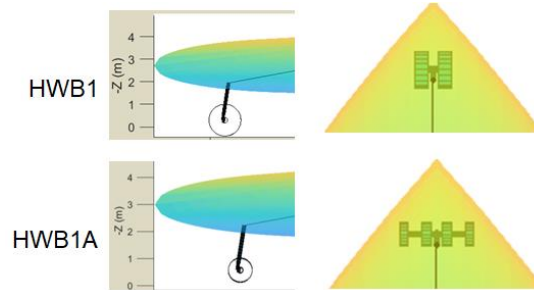


**Fig. 3 HWB1 and HWB1A NLG size and stowage.**

Required axle dimensions were determined based on the maximum bending stress at the leg-axle connection point, using a yield stress of 250 MPa and a safety factor of 2. This method enables a rough weight prediction for this component for each design. The results of the axle design for HWB1 and HWB1A are shown in Table 5 compared to the NBC.

**Table 5 Axle design details for NBC and HWB1/HWB1A.**

	NBC NLG	NBC MLG	NLG HWB1	NLG HWB1A	HWB1/HWB1A MLG
Diameter, m	0.114	0.263	0.237	0.272	0.233
Thickness, m	0.006	0.013	0.012	0.014	0.012
Axle Width, m	0.50	0.91	0.90	0.90	0.90
Outer Width, m	-	-	-	1.80	-
Mass, kg	8	73	59	78	57

For the oleo shock absorber design, first the design loading conditions were considered. During typical operations, largest oleo forces occur during braking for the NLG and landing for the MLG. GearSim’s Oleo Design Toolbox applies basic assumptions of the oleo performance to calculate force as a function of stroke and recoil/damping values. For this work, recoil values are equal to the compression values plus  $2e5 \text{ N s}^2/\text{m}^2$  in the absence of better data. NLG and MLG design load and equivalent sprung mass are shown below in Table 6. The results for the NLG oleo design are shown in Fig. 4 in terms of a spring force vs. oleo closure, and damping coefficient vs. oleo closure. Fig. 4 also shows how the spring force lines up with the design load. The pitch inertia of HWB1 was scaled from NBC, so the design mass for these two designs and the minimum coefficient damping coefficient are similar.

**Table 6 NLG and MLG oleo design load and sprung mass.**

NLG Oleo Design: Braking Case			MLG Oleo Design: Landing Case		
Aircraft	NBC	HWB1	Aircraft	NBC	HWB1
Design Load, N	133,340	305,381	Design Load, N	360,518	235,120
Design Mass, kg	37,204	34,878	Design Mass, kg	36,750	23,967
Diameter, in	5.04	7.64	Diameter, in	8.29	6.69

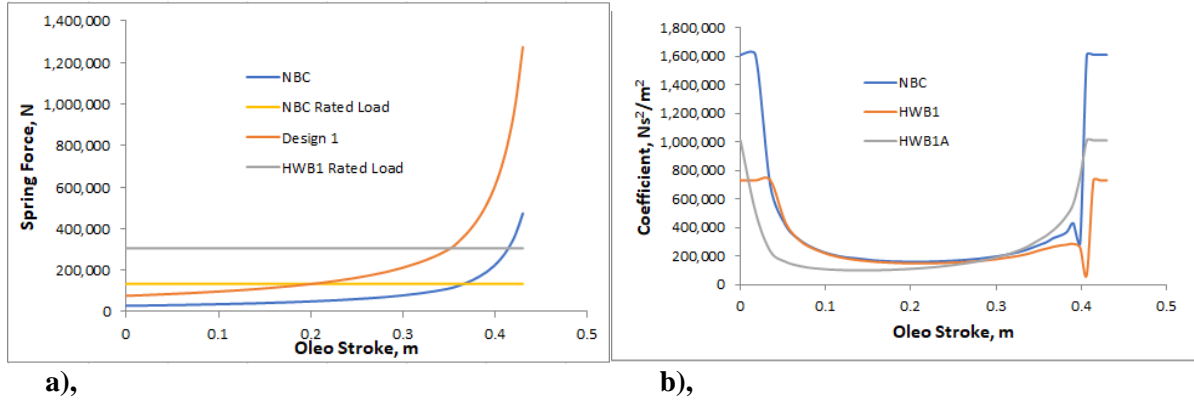


**Fig. 4 NLG oleo spring force (a) and damping (b) for NBC and HWB1/HWB1A.**

Next, the leg diameters were resized to fit new oleo design, with the results shown in Table 7. The leg weight was estimated not including a drag or side brace, and assuming a thickness to radius ratio of 10%. Total weight was summed for the NLG and MLG subsystem components. Compared to the NBC, these HWB designs are heavier, because they essentially have three load-bearing components instead of only two. Further design optimizations are required for HWB1 and HWB1A; while the NBC is based on an optimized, tried-and-true design.

**Table 7 NLG and MLG leg design and total weight estimation.**

NLG Leg Design				MLG Leg Design			
Aircraft	NBC	HWB1	HWB1A	Aircraft	NBC	HWB1	HWB1A
Oleo Diameter, m	0.128	0.194	0.194	Oleo Diameter, m	0.211	0.170	0.170
Lower Leg Diameter, m	0.142	0.216	0.216	Lower Leg Diameter, m	0.234	0.189	0.189
Lower Leg Thickness, m	0.007	0.011	0.011	Lower Leg Thickness, m	0.012	0.009	0.009
Upper Leg Diameter, m	0.158	0.240	0.240	Upper Leg Diameter, m	0.260	0.210	0.210
Upper Leg Thickness, m	0.008	0.012	0.012	Upper Leg Thickness, m	0.013	0.010	0.010
Leg Mass, kg	41	94	94	Leg Mass, kg	174	114	114
Total Mass, kg	213	838	661	Total Mass, kg	784	503	503
<b>Total Landing Gear Mass, kg</b>				<b>997</b>	<b>1,341</b>	<b>1,165</b>	

## VI. Performance Comparison

The landing, braking, and steering performance of the HWB1 and HWB1A models were then compared with the NBC. For landing, the aircraft response is shown in Fig. 5.

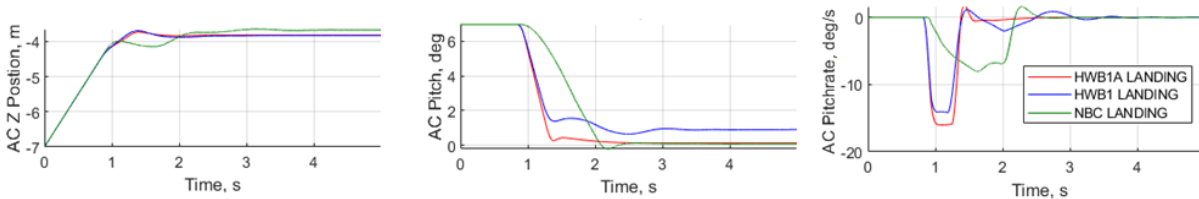


**Fig. 5 Simulated aircraft response during landing.**

The tire force response from the landing simulations are shown in Fig. 6. MLG tire X forces are similar for each configuration but spin-up is faster for the NBC case. MLG tire Z forces are similar between HWB1 and HWB1A, but higher for the NBC. A higher NBC MLG force is expected from the static load distribution as less weight is carried by the NLG for the NBC. A small bounce in the NBC results show that oleo energy absorption effectiveness could improve in this case, or the maneuver settings could be altered to achieve a smoother touch-down. For the NLG, the tire forces for the 2-wheel HWB1 are significantly higher than for the NBC, again expected from the load distribution as well as the increased nose-down pitch rate on touchdown. NLG tire forces for the 4-wheel HWB1A are more in line with NBC tire loads.

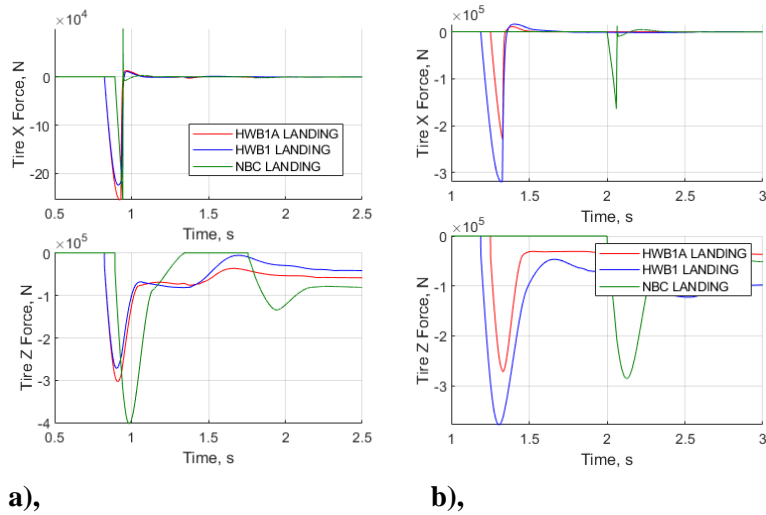


**Fig. 6 Landing simulation tire forces for MLG (a) and NLG (b).**

The oleo responses from the landing simulations are shown in Fig. 7. Oleo designs effectively absorb the landing energy in each case. The bounce shown in the NBC results highlight the advantage of a natural derotation for HWBs. For the NLG, a higher stiffness of the NLG tires in the four-wheel case results in lower energy absorption for the oleo. An increased final NLG oleo closure for the HWBs may be an indication to slightly raise the NLG position; this highlights the iterative design process for LG and the need to revisit the design as the subsystems become more well-defined.

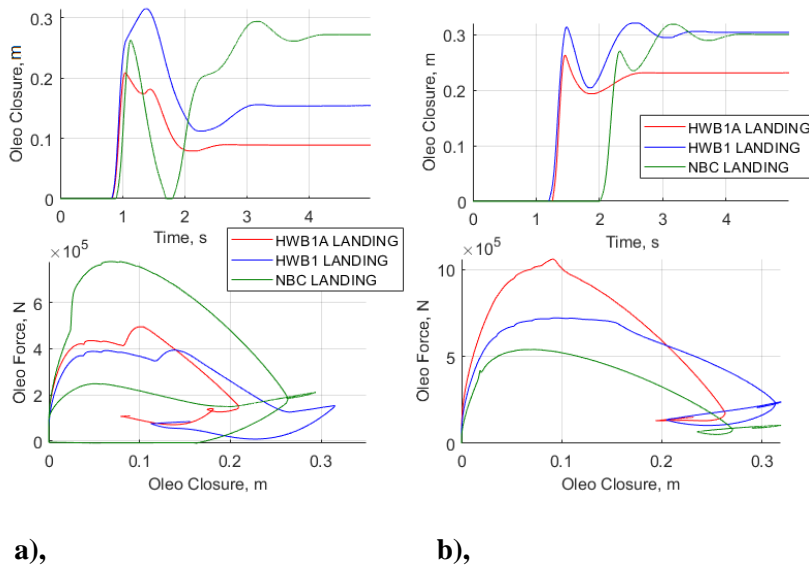


**Fig. 7 Landing simulation oleo response for MLG (a) and NLG (b).**

The leg force response for the landing simulations is shown in Fig. 8. MLG landing loads are of similar magnitude for all cases, with slightly higher vertical loads for the NBC. Note the spring-back (X force) loads are smooth because the leg flexibility is omitted from this simulation. The lower load on the MLG is due to the static load distribution and more vertical motion as the aircraft rotates downwards. The higher pitch-down landing response of the HWBs also quickly reduces the aircraft lift and alleviates load on the MLG.

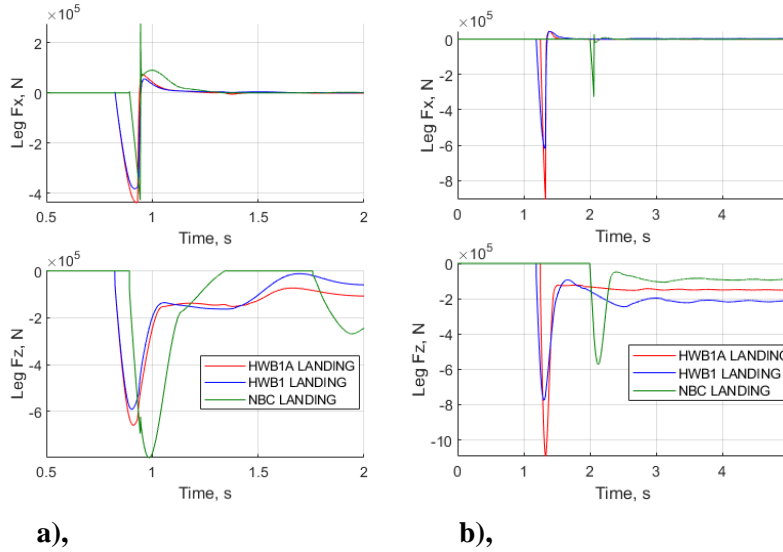


**Fig. 8 Landing simulation leg forces for MLG (a) and NLG (b).**

The NBC, HWB1, and HWB1A were then subjected to a deceleration case. When examining results for the HWB1A, a shimmy vibration was observed with oscillation of the lateral leg force and steering angle as shown in Fig. 9. Different NLG properties between HWB1 and HWB1A led to a lightly damped vibration of the steering collar for HWB1A. Steering torque control system gains were increased by a factor of 2.5 for HWB1A to alleviate this shimmy vibration. This issue shows how important a systems-level analysis tool is at the early stages of the design; if it was missed it would be a costly mistake! A dedicated shimmy analysis of the design change was not possible in the scope of this design study.

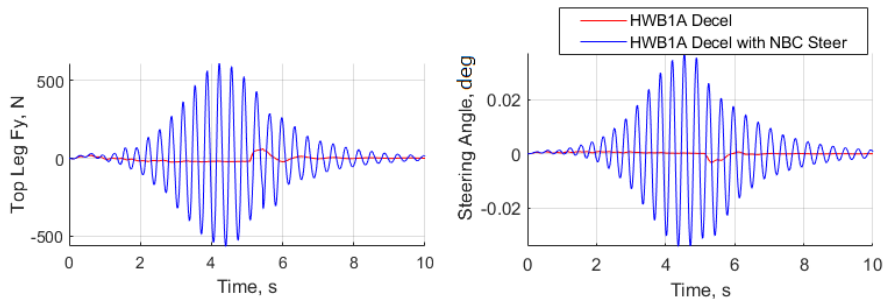


**Fig. 9 Shimmy vibration observed with HWB1A for deceleration case.**

To examine the response of the HWB1 and HWB1A in braking, simulations were set up for each case and compared to the NBC in Fig. 10. For this case, the braking simulation begins at a quasi-static initial condition of 10 m/s on the runway and slows to 2 m/s over 5 seconds. The acceleration rate of  $2 \text{ m/s}^2$  is typical of a braking effort after landing. GearSim's Taxi Path and Pilot Module adjusts the braking command based on the velocity error between the aircraft velocity and prescribed velocity, and GearSim's antiskid model adjusts the braking torque based on the error between the desired slip ratio and commanded slip ratio. Antiskid properties were adjusted for all models to accommodate for differing MLG tire diameters. Because of the control systems maintaining a specified deceleration profile, a very similar MLG drag force  $F_x$  can be observed in all cases. The slip ratio was significantly higher for the HWB cases to achieve the same braking force. For moderate braking, the different LG arrangement does not adversely impact braking performance due to the antiskid system. NLG braking forces were consistent with oleo design predictions. Overall, the braking performance comparison indicates that HWB1 and HWB1A have similar braking performance but with lowered maximum braking acceleration due to maximum slip ratio limitations.

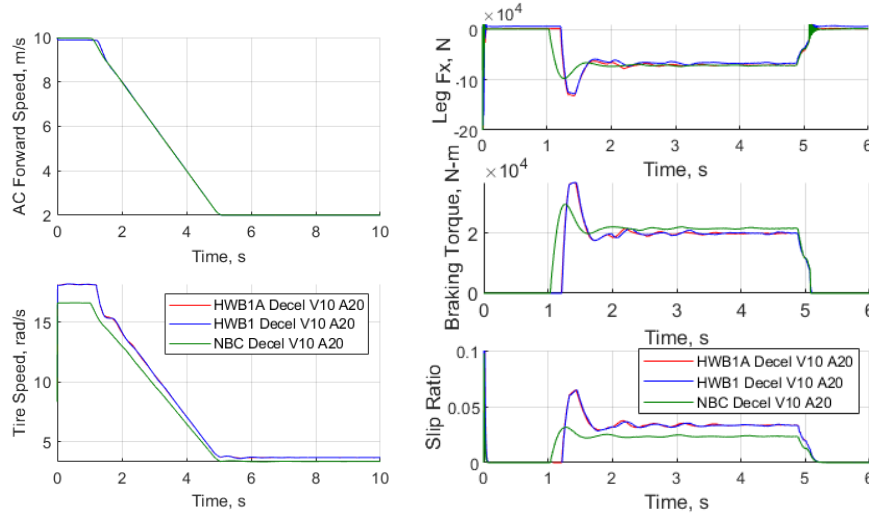


**Fig. 10 Braking response for moderate braking simulations.**

Finally, a steering performance comparison was conducted for the NBC, HWB1, and HWB1A models based on a moderate steering simulation as shown in Fig. 11. A 15 degree steering angle command was applied to each aircraft from a quasi-static initial condition on the runway at 5 m/s forward velocity. The HWB1A has increased steering system control gains, so the initial higher transient response is expected (1 to 2 seconds). Increased loads on the NLG for HWB1 and HWB1A leads to a higher lateral force. The decreased wheelbase of HWB1 and HWB1A compared to the NBC also improves the turning radius for these aircraft. The 4-wheel HWB1A had significantly higher lateral loads, even in the steady-state turn, resulting in a very high yaw rate for this case.

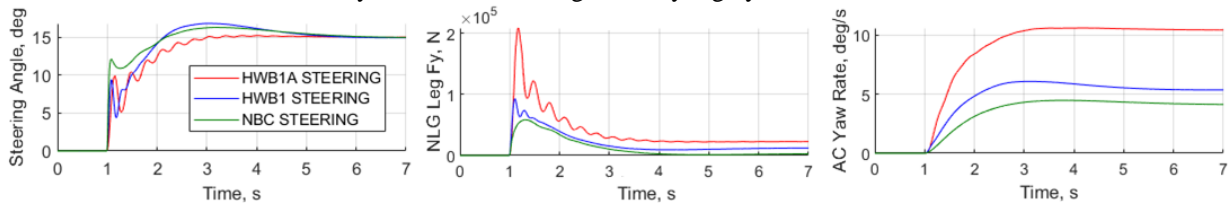


**Fig. 11 Steering response for moderate steering simulations.**

## VII. Conclusion

This work presents designs and requirements for several realistic HWB landing gear. Detailed whole aircraft and LG simulations were conducted for these models using SDI's GearSim software. Comparing the design results between different classes and sizes of HWB aircraft revealed how the requirements for the landing gear change for these aircraft.

This study provides a realistic picture of the landing gear for several popular HWB designs. Overall, the study indicates that LG design challenges for HWB can be overcome and are not a barrier. LG design is an iterative

process, and this study is just the first iteration. Including LG in the early stages of the design is important to avoid unfavorable interaction problems such as shimmy.

This work divided the HWB aircraft into three categories for LG design. In the smallest category, (e.g. B737/A320), there is limited MLG stowage capacity, potentially leading to aft placement of the MLG. In the midsize category, (e.g. B777/A380), there is additional stowage capacity in a second deck below the passenger deck, and nearly identical LG design to conventional aircraft. For the very large category, with 750 passengers, 4-wheel NLG and four 6-wheel MLG, there are many options for the LG layout, with tire loads being manageable when compared to today's large wide-body aircraft. Further work can understand the unique considerations for these large HWB landing gear.

For small HWBs with limited MLG stowage capacity, the MLG is placed aft, behind the main passenger compartment, leading to additional aircraft and LG design requirements. The flight control system (FCS) can be adjusted to reduce increased nose-down pitch rate on touchdown, or adjusted to take advantage of the natural derotation effect created by the aft MLG placement. The differing static load distribution, with much higher load on the NLG and slightly lower MLG loads, leads to the consideration of a 4-wheel NLG, for its reduced overall weight, the lower stowage capacity due to smaller tires, and the available lateral stowage capacity for HWB aircraft. The increased NLG load may require additional stiffness and damping in the NLG steering system to prevent shimmy. Decreased MLG loads limit the maximum braking acceleration but otherwise do not affect the braking system performance. The steering performance of these HWB is expected to improve due to the higher NLG load and lateral forces combined with the reduced wheelbase.

SDI is working on a structural design module for GearSim that will incorporate a detailed structural model of the landing gear and provide estimates of weight at the early design stage. In future work, this structural weight optimization process can be applied to these designs to provide a more accurate weight estimate that can be used in future preliminary HWB and FW design studies. SDI would also like to acknowledge Ayden Young for his contribution to this effort when this endeavor was in its early stages.

## References

- [1] R. Martínez-Val, "Flying Wings. A New Paradigm for Civil Aviation?".  
doi: 10.14311/914
- [2] D. P. Raymer, Aircraft Design: A Conceptual Approach, p. 1062.  
doi: 10.2514/4.104909
- [3] E. Torenbeek, Advanced Aircraft Design, 2012.  
doi: 10.1017/S0001924000010423
- [4] P. Okonkwo and H. Smith, Review of evolving trends in blended wing body aircraft design, vol. 82, Elsevier Ltd, 2016, pp. 1-23.  
doi: 10.1016/j.paerosci.2015.12.002
- [5] Z. CHEN, M. ZHANG, Y. CHEN, W. SANG, Z. TAN, D. LI and B. ZHANG, Assessment on critical technologies for conceptual design of blended-wing-body civil aircraft, vol. 32, Chinese Journal of Aeronautics, 2019, pp. 1797-1827.  
doi: 10.1016/j.cja.2019.06.006
- [6] R. Martínez-Val and E. Shoep, Flying Wing versus Conventional Transport Airplane: The 300 Seat Case, 2000.
- [7] R. H. Liebeck, Design of the Blended Wing Body Subsonic Transport, vol. 41, American Institute of Aeronautics and Astronautics, 2004, pp. 10-25.  
doi: 10.2514/1.9084
- [8] P. Okonkwo, "Conceptual Design Methodology for Blended Wing Body Aircraft".
- [9] R. Martínez-Val, E. Pérez, P. Alfaro and J. Pérez, Conceptual design of a medium size flying wing, vol. 221, IMECHE, 2007, pp. 57-66.  
doi: 10.1243/09544100JAERO90
- [10] M. Potsdam, M. Page, R. Liebeck, M. Potsdam, M. Page and R. Liebeck, Blended Wing Body analysis and design, American Institute of Aeronautics and Astronautics, 1997.  
doi: 10.2514/6.1997-2317
- [11] M. Brown and R. Vos, Conceptual Design and Evaluation of Blended-Wing-Body Aircraft, American Institute of Aeronautics and Astronautics Inc, AIAA, 2018.  
doi: 10.2514/6.2018-0522
- [12] T. Saeed, W. Graham, H. Babinsky, J. Eastwood, C. Hall, J. Jarrett, M. Lone and K. Seffen, Conceptual Design for a Laminar Flying Wing Aircraft, American Institute of Aeronautics and Astronautics, 2009.  
doi: 10.2514/6.2009-3616
- [13] A. Bolsunovsky, N. Buzoverya, I. Chernyshev, B. Gurevich and A. Tsyganov, Arrangement and Aerodynamic Studies for Long Range Aircraft in "Flying Wing" Layout, 2014.
- [14] D. Espinal, B. Lee, H. Sposato, D. Kinard, J. Dominguez, G.-c. Zha and H. Im, Supersonic Bi-Directional Flying Wing, Part II: Conceptual Design of A High Speed Civil Transport, American Institute of Aeronautics and Astronautics, 2010.  
doi: 10.2514/6.2010-1393
- [15] M. S. A. Voß, Design and Structural Optimization of a Flying Wing of Low Aspect Ratio Based on Flight Loads, 2020.  
doi: 10.14279/depositonce-9858
- [16] T. W. Laughlin, A Parametric and Physics-Based Approach to Structural Weight Estimation of the Hybrid Wing Body Aircraft, 2013.  
doi: 10.2514/6.2013-1082
- [17] F. H. Gern, Finite Element Based HWB Centerbody Structural Optimization and Weight Prediction, 2013.  
doi: 10.2514/6.2012-1606
- [18] L. U. Hansen, W. Heinze and P. Horst, Blended wing body structures in multidisciplinary pre-design, vol. 36, 2008, pp. 93-106.  
doi: 10.1007/s00158-007-0161-z
- [19] S. Cumnantip, "LANDING GEAR CONCEPTUAL DESIGN AND STRUCTURAL OPTIMIZATION OF A LARGE BLENDED WING BODY CIVIL TRANSPORT AIRCRAFT," 2015.
- [20] A. L. Bolsunovsky, N. P. Buzoverya, B. I. Gurevich, V. E. Denisov, A. I. Dunaevsky, L. M. Shkadov, O. V. Sonin, A. J. Udzhuhu and J. P. Zhurihin, "Flying wing - problems and decisions," 2001.  
doi: 10.1016/S1369-8869(01)00005-2
- [21] M. A. Page, E. J. Smetak, and S. L. Yang. "Single-Aisle Airliner Disruption with a Single-Deck Blended-Wing-Body," in *31st Conference of the International Council of the Aeronautical Sciences*, Belo Horizonte, Brazil, 2018.
- [22] C. L. Nickol, Hybrid Wing Body Configuration Scaling Study, 2012.  
doi: 10.2514/6.2012-337

- [23] P. W. Richards and A. J. Erickson, "Dynamic Ground Loads Analysis Using Detailed Modeling of Landing Gear and Aircraft Aeroservoelastics," in *AIAA SciTech Forum*, San Diego, CA, 2019.  
doi: 10.2514/6.2019-0759
- [24] M. McDonald, P. W. Richards, M. Walker and A. J. Erickson, "Carrier Landing Simulation using Detailed Aircraft and Landing Simulation," in *AIAA SciTech Forum*, Orlando, FL, 2020.  
doi: 10.2514/6.2020-1138
- [25] P. W. Richards, B. M. Tate, M. Kuwayama, I. Kurino and H. Isshiki, "Aircraft Taxi Simulations with Detailed Aircraft and Landing Gear Modeling," in *AIAA SciTech Forum*, National Harbor, MD, 2023.
- [26] P. Birtles, *Boeing 777: Jetliner for a New Century*, 1998.
- [27] GoodYear Aviation, "2022 GoodYear Aviation Data Book," 2022. [Online]. Available: <https://www.goodyearaviation.com/resources/pdf/Aviation-Databook-2022.pdf>.